Open Access

Distributed Temperature Sensing Using Stimulated-Brillouin-Scattering-Based Slow Light
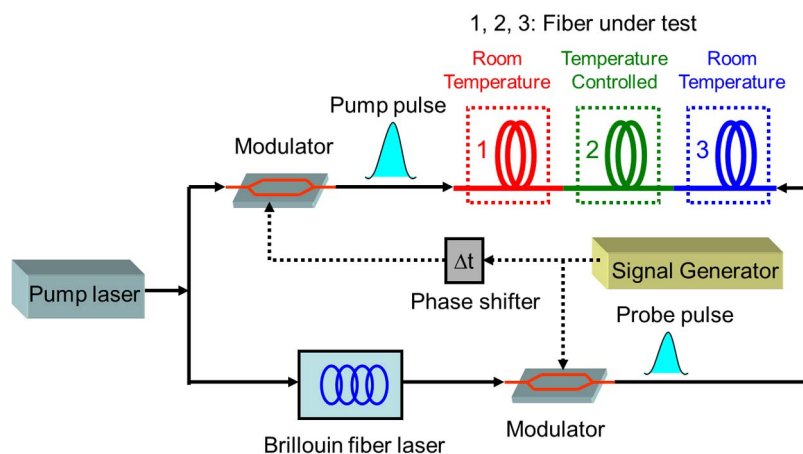
Liang Wang
Bin Zhou
Chester Shu, Senior Member, IEEE
Sailing He, Fellow, IEEE

Distributed Temperature Sensing Using Stimulated-Brillouin-Scattering-Based Slow Light

Liang Wang,[1,2] **Bin Zhou,**[1] **Chester Shu,**[2] *Senior Member, IEEE*, **and Sailing He,**[1,3,4] *Fellow, IEEE*

[1]Centre for Optical and Electromagnetic Research, South China Academy of Advanced Optoelectronics, South China Normal University, Guangzhou 510631, China
[2]Department of Electronic Engineering and Center for Advanced Research in Photonics, The Chinese University of Hong Kong, Shatin, Hong Kong
[3]Centre for Optical and Electromagnetic Research, State Key Laboratory for Modern Optical Instrumentation, Zhejiang University, Hangzhou 310058, China
[4]Division of Electromagnetic Engineering, School of Electrical Engineering, Royal Institute of Technology, 100 44 Stockholm, Sweden

Abstract: Distributed temperature sensing has been achieved by spatially resolved measurement of the probe time delay resulted from stimulated-Brillouin-scattering slow light. The temperature of a particular fiber section can be monitored by setting an appropriate relative delay between the pump and probe pulses. By controlling the relative delay, we have achieved distributed profiling of the temperature along the whole sensing fiber. This scheme provides an alternative way for distributed temperature sensing with the potential of real-time temperature monitoring. A relatively high-temperature resolution of 0.7 °C is obtained.

Index Terms: Distributed temperature sensing, stimulated Brillouin scattering, slow light.

1. Introduction

Fiber sensors have been widely used in structural health monitoring to determine changes in temperature, strain, and pressure. The sensors offer the advantages of small size, immunity to electromagnetic interference, and survivability under harsh environments. Among different types of sensors, Brillouin distributed fiber sensors have attracted considerable attention [1]–[11]. The amount of Brillouin frequency shift is related to the acoustic velocity and the fiber refractive index, which are dependent on both the temperature and the strain. Based on this principle, Brillouin sensors have been demonstrated using the Brillouin optical time-domain reflectometer (BOTDR) configuration [1]. In addition, owing to the temperature and strain dependence of the frequency shift, the Brillouin gain or loss is also temperature and strain dependent, giving rise to Brillouin gain/loss based sensing configurations such as Brillouin optical time-domain analysis (BOTDA) [2]–[6] and Brillouin optical frequency-domain analysis (BOFDA) [7], [8]. The technique of Brillouin optical correlation-domain analysis (BOCDA) [9]–[11] has been used for Brillouin sensors to achieve centimetric resolution. These conventional Brillouin sensors are promising for long distance sensing while offering a high resolution.
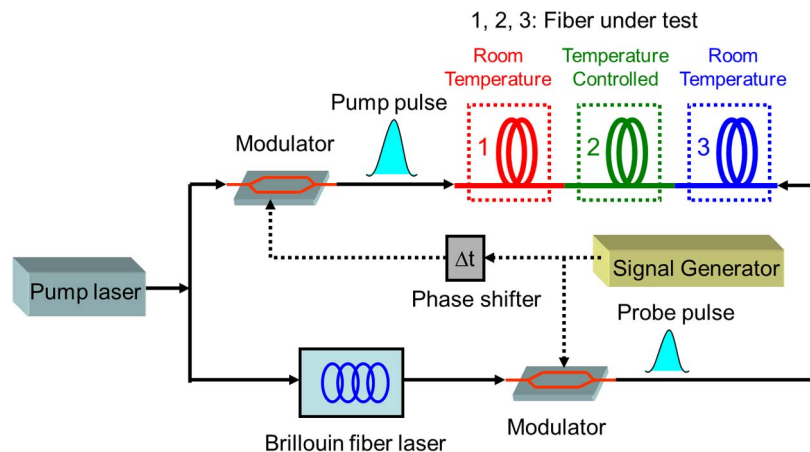
Fig. 1. Schematic illustration of the proposed distributed temperature sensing scheme based on SBS slow light.

Apart from its applications in optical sensing, stimulated Brillouin scattering (SBS) has been actively pursued for slow light in fibers [12]–[20]. Many applications have been found in communications, such as optical synchronization, optical multiplexing/demultiplexing, and optical equalization [19]. However, despite these applications, slow light is rarely associated with temperature or strain sensing. Recently, we have demonstrated the feasibility of fiber temperature sensing taking advantage of SBS based slow light [21], [22], which is considered elsewhere as a penalty in traditional sensors [17]. The temperature was monitored by measuring the delay time of the probe pulse. A temperature resolution better than 1 °C was obtained. In this work, we further demonstrate the use of SBS slow light for distributed temperature sensing. By operating the pump in a pulsed mode and by controlling the relative delay time between the pump and probe pulses, dynamic measurement [23] can be obtained at any particular fiber location. That is to say, instead of static measurement of temperature or strain like conventional Brillouin sensors, this approach offers a potential means for fast dynamic real-time monitoring of a particular position. In our case, the fiber under test is 370 m, leading to a repetition measurement frequency of 0.54 MHz. In addition, for a fiber length up to several tens of kilometers, the repetition frequency is on the order of kHz. The temperature variation should be within a certain range ($\sim$25 °C in our case) where the probe frequency falls within the SBS gain bandwidth. On the other hand, for the measurement on static temperature distribution along the whole fiber, one just needs to combine the results obtained at different relative delay times.

2. Principle and Experimental Setup

Fig. 1 shows the working principle of our distributed temperature sensing scheme. A CW pump laser is divided into two branches. The upper branch is used for the generation of pump pulses for SBS slow light, whereas the lower branch is applied as the pump for a Brillouin fiber laser. The fiber laser output is modulated to produce a probe pulse for SBS slow light. The probe pulse operates at the Stokes frequency of the fiber in the Brillouin laser cavity, which is of the same type of fiber under test. The arrangement provides automatic spectral alignment for wavelength transparent slow light [18]. In our demonstration, we divide the fiber under test into three sections. The temperature of the middle section (section 2) is varied, and the other two sections (sections 1 and 3) are maintained at the room temperature. The slow light effect is introduced in the fiber under test. The duration and the length of interaction are determined by the widths of the counter-propagating pump and probe pulses. If the two pulses cross at sections 1 or 3, the probe will experience the maximum delay because its frequency is automatically aligned to the Stokes frequency in the sections. If the two pulses cross at section 2, the probe pulse will experience a slow light delay dependent on the fiber
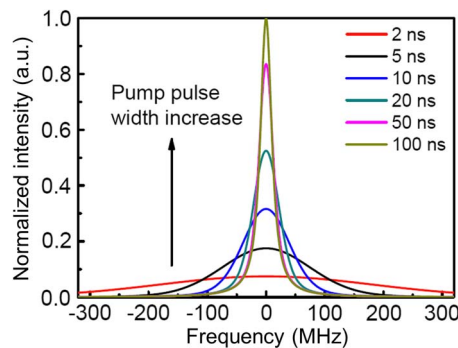
Fig. 2. Simulated Brillouin gain spectra for Gaussian shaped pump pulse with different widths.

temperature. The underlying principle is that the Brillouin frequency shift in section 2, hence the SBS gain of the probe, is determined by the temperature. By controlling the relative delay between the pump and probe pulses, the crossover point can be set at any arbitrary position along the fiber. One can monitor a fixed crossover point in real time. Certainly, through measuring the SBS probe delay for different crossover points, the temperature distribution along the whole sensing fiber can be observed.

In our scheme, both the pump and probe are pulses; thus, the choice of the pulse width combination would be important. This is because the spatial resolution of our sensing technique is determined by the overlapping distance of the pump and probe pulses along the fiber where the interaction takes place [24]. Specifically, it is obtained from the product of the group velocity and the average of the pump and probe pulse widths. The spatial resolution can be improved by using shorter pulses, but there are several factors needed to be considered. On one hand, the situation to reduce the pump pulse width is somewhat complex. According to Ref. [14], the Brillouin gain spectrum is the convolution of the pump spectrum and the intrinsic Brillouin gain spectrum. Fig. 2 shows the simulated Brillouin gain spectrum for Gaussian shaped pump pulse with different widths. The intrinsic Lorentzian Brillouin gain bandwidth is assumed to be ~40 MHz in single mode fiber (SMF). We can clearly see that the decrease of the pump pulse width will give rise to a reduction of the peak gain and broadening of the gain bandwidth. As the pump pulse width is less than 100 ns, the transient regime of SBS should be considered [25]. When the width is shorter than the phonon lifetime (typical value < 10 ns in SMF), SBS eventually ceases to occur (2 ns and 5 ns cases in Fig. 2). Hence, it is necessary to raise the pump power to maintain the same gain and thus the temperature sensitivity. However, a large pump power will degrade the sensing performance due to the occurrence of other nonlinear effects such as self-phase modulation. On the other hand, a shorter probe pulse will imply a broader spectral width, resulting in pulse distortion due to the limited SBS gain bandwidth [14]. The pulse distortion affects the accuracy and hence limits further improvement in the spatial resolution. The pump spectral broadening technique may be applied for the delay of picosecond probe pulses [14]–[16]. Similarly, it will lead to a decrease in temperature sensitivity unless higher pump power is used to compensate for the decreased gain coefficient. Therefore, those joint effects need to be comprehensively considered, and the choice of the optimal pulse width is strongly dependent on the practical applications. We can take a pulsed pump with a width of 20 ns as an example to understand those trade-offs. After the convolution, the gain bandwidth is about 90 MHz, which can support the delay of ~11 ns probe pulse. In this pump/probe pulse width combination, the spatial resolution is ~3.1 m. Although this combination offers relatively high spatial resolution, it needs higher pump power to achieve the same gain when compared with that for 100 ns pulsed pump, as shown in Fig. 2. In addition, it sacrifices some accuracy of the scheme since the Brillouin gain bandwidth is just enough to delay the probe pulse. So, in practical application, if the high spatial resolution is more important than the accuracy and temperature sensitivity, one can employ shorter pulse combination, while if the accuracy and sensitivity are the concerns, one should sacrifice the spatial resolution and use wider pulse combination. The optimal
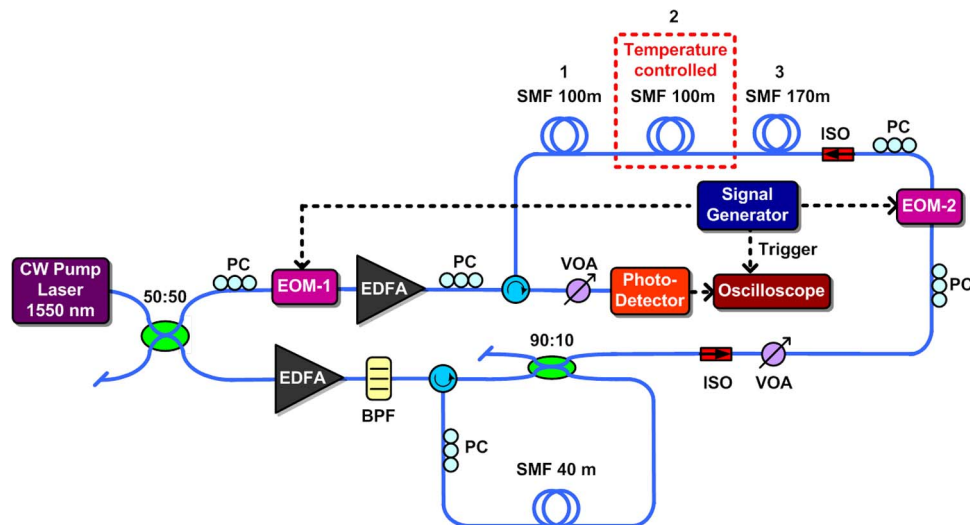
Fig. 3. Experimental setup for distributed temperature sensing. EOM: electro-optic intensity modulator; EDFA: erbium-doped fiber amplifier; PC: polarization controller; VOA: variable optical attenuator; BPF: band pass filter; SMF: single mode fiber; ISO: isolator.

width combination depends on the requirements in practical situation. In our experiment, we just use 100/50 ns pump/probe pulse width combination for the demonstration of our concept. The spatial resolution is ~15 m and is only a conservative estimation since the calculated distance includes the whole duration of partial and complete overlapping of pulses.

The experimental setup is shown in Fig. 3. The composition of the fiber under test is two sections of 100 m SMFs and one section of 170 m SMF. The lengths of the fiber under test for all the three sections are not intentionally selected. Longer fiber length can also be adopted in our scheme, as long as the relative time delay between the pump and probe pulses can be set to cover all the sensing points along the fiber and appropriate in-line Raman amplifiers [5] are used to compensate the attenuation. The temperature of the middle 100 m SMF section is varied during the experiment, while the other two sections are kept at the room temperature. A CW pump laser at 1550 nm is split into two branches. The upper branch is intensity-modulated by an electro-optic intensity modulator (EOM-1) to provide a 100 ns pump pulse. After amplification, the polarization of the pump pulse is optimized with a polarization controller. Alternatively, a polarization scrambler can be used to minimize polarization-induced noise [26] as was demonstrated with strain sensing [27]. The lower branch is amplified to pump a Brillouin fiber laser constructed with 40 m SMF. Longer fiber length can be adopted in the Brillouin fiber laser cavity, but it should be carefully chosen to make the laser output stable with small intensity noise. The output power of the laser is controlled by a variable optical attenuator to facilitate the amplification and delay of the probe. The laser output is then intensity-modulated by EOM-2 to produce a 50 ns probe pulse. The pump and probe pulses are synchronized with a repetition period of 20 μs. Their relative delay can be controlled by the electrical signal generator. The relative delay determines the crossover point of the two counter-propagating pulses in the fiber under test, where SBS slow light is introduced. The probe pulse is then measured by a photodetector connected to an oscilloscope to determine the SBS slow light delay.

3. Results and Discussions

Fig. 4 plots the profiles of the delayed probe pulses when the crossover of the pump and probe occurs at different positions along the fiber: length L $=$ 50 m, 150 m, and 250 m, corresponding to crossover at sections 1, 2, and 3, respectively. In this measurement, the temperature of section 2 is fixed at room temperature (22.4 °C). The red, green, and blue curves in Fig. 4 show that the probe pulses experience almost the same amount of delay. The result is expected as the three sections of
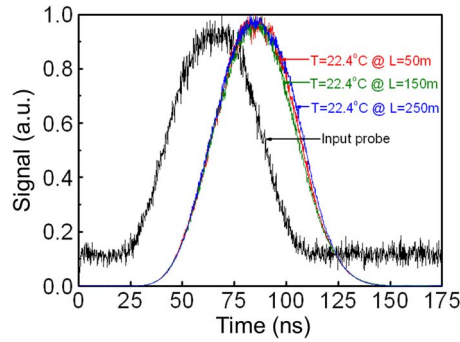
Fig. 4. Measured output probe pulses for three different crossover (sensing) points at section 1 (L = 50 m), section 2 (L = 150 m), and section 3 (L = 250 m) when section 2 is maintained at room temperature.
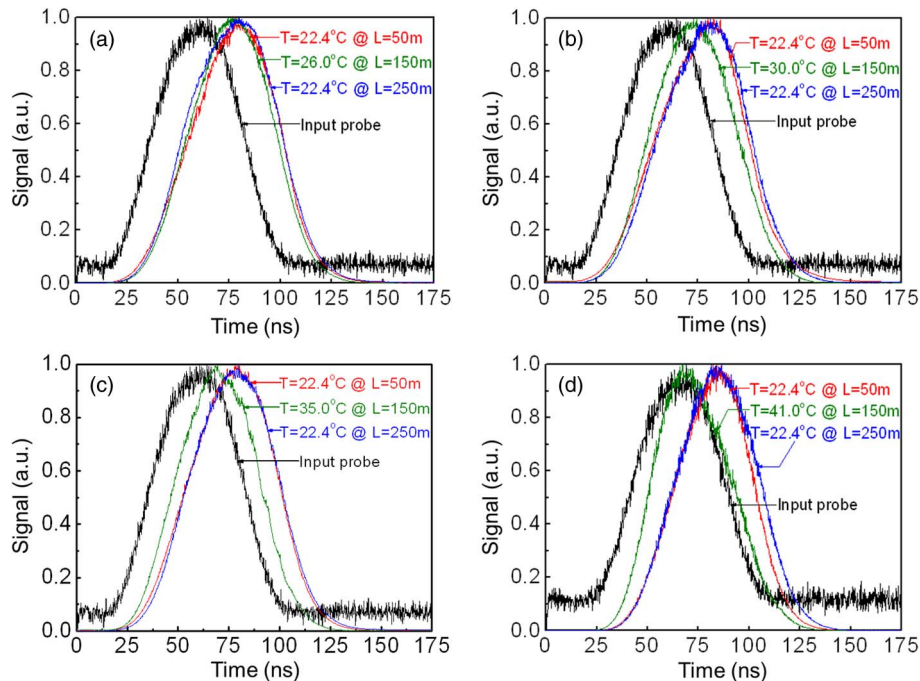

Fig. 5. (a)–(d) Measured output probe pulses for crossover (sensing) points at the three sections of fibers when section 2 is maintained at (a) 26.0, (b) 30.0, (c) 35.0, and (d) 41.0 °C.

the fiber under test are all maintained at the room temperature. The achievable maximum gain is ~20 dB, and the maximum delay time is ~20.0 ns. The output profiles appear to be smoother than the input one because the number of average values used in the measurement is four times that of the input. Next, we change the temperature of section 2 to 26.0, 30.0, 35.0, and 41.0 °C and repeat the measurement. The delayed probe pulses are shown in Fig. 5. The SBS delay is almost unchanged (~20.0 ns, shown as the red and blue curves) for the cases when the crossover occurs at section 1 or 3. However, the delay is reduced when the crossover is at section 2 as the temperature is increased. The results are displayed as the green curves. From both Figs. 4 and 5, at fixed crossover points (fiber length L=50 m, 150 m, and 250 m), we can expect the potential of this scheme for dynamic real-time monitoring. A slight distortion of pulses is observed and is attributed mainly to the limited SBS gain bandwidth. The signal-to-noise ratio (SNR) can be further improved by increasing the averaging times (64 averaging times in our results) on the oscilloscope.
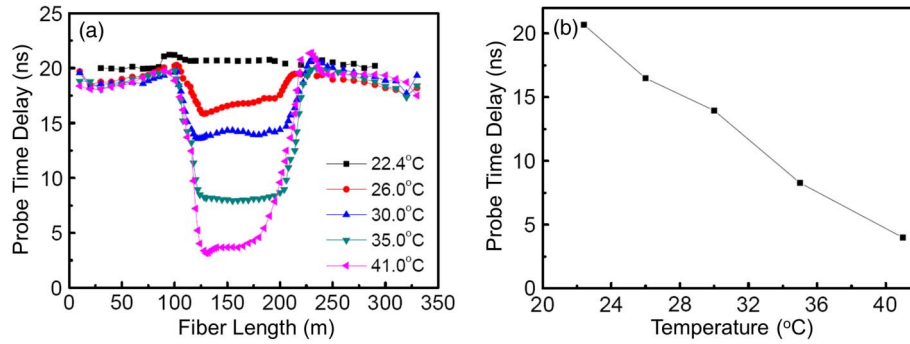
Fig. 6. (a) Delay time of the probe pulse when the pump and probe pulses cross over at different positions along the sensing fiber. The temperatures of section 2 are set at 22.4, 26.0, 30.0, 35.0, and 41.0 °C, respectively; (b) average values of the SBS probe delay at section 2 as derived from the data in (a).

To obtain the static temperature distribution along the sensing fiber, we also measure the SBS probe delay for other crossover positions. The measurement steps vary from 2 to 10 m, depending on the temperature gradient at the particular position. For each set of measured data along the sensing fiber, an average was taken over every five measurement positions for three times, in order to minimize the effect of noise. Fig. 6(a) shows the SBS probe delay for different crossover positions along the fiber under test when section 2 is maintained at five different temperatures. One can clearly distinguish the delay time at section 2 from those at sections 1 and 3. Note that the asymmetry of the curves would origin from the polarization-induced noise since we manually adjust the polarization states of the pump and probe pulses by PC. Hence, the polarizations may not be optimized at some positions. Fig. 6(b) shows the average values (20.68, 16.49, 13.95, 8.28, and 3.99 ns) of the SBS probe delay at section 2 versus the five temperatures. Because of the same pump pulse width and same type of sensing fiber as that used in the 2 m SMF configuration reported in Ref. [21], here, for simplicity, we do not further increase the temperature until the delay becomes zero (this temperature defines the sensing range). The temperature sensing range is approximately ~ 25 °C from the room temperature, similar to that of the 2 m SMF configuration reported in Ref. [21]. Like most of the approaches [2], [4], [6], [10], [11] used in calculating temperature/strain resolution, we obtain the temperature resolution from the ratio of the measurement error and the temperature sensitivity. The temperature sensitivity is the slope of the curve in Fig. 6(b), and it is 0.90 ns/°C. Similar to that in Ref. [21], the measurement error can be approximated by the root-mean-square (RMS) deviations between the experimental data and the calculated results. The experimental data are depicted in Fig. 6(b), while the calculated time delay are obtained using the equations in Ref. [21, eqs. (1) and (2)]. The parameters used here are as follows: $\alpha = 1.07$ MHz/°C, $T_0 = 22.4$ °C, $\Gamma_B/2\pi = 50$ MHz, and $\Delta t_m = 20.68$ ns. Therefore, the RMS deviation between the experimental data and the calculated delay is found to be ~ 0.60 ns. Hence, a temperature resolution of 0.7 °C is obtained. The resolution can be enhanced by increasing the temperature sensitivity or reducing the measurement error. To improve the sensitivity, one can increase the pump power to enhance the SBS gain and thus the time delay of the probe pulse. To reduce the measurement error, several factors should be considered. The error can originate from pump power fluctuations, polarization-induced pulse distortion [26], and intensity noise transferred from the instability of the Brillouin fiber laser [18]. These factors can result in fluctuations of the probe pulse delay and hence inaccuracy of the measurement. Therefore, a laser with a steady output power, a polarization scrambler, and a stable Brillouin fiber laser cavity should be employed together with the averaging function of the oscilloscope. In addition, probe pulse distortion due to limited SBS gain bandwidth will cause difficulties in determining the delay time, hence contributing to measurement error. Wider probe pulse will experience less distortion and improve the accuracy; however, the spatial resolution will be sacrificed. A trade-off should thus be adopted according to practical considerations.

It is worth mentioning that the measurable range of temperature can be enlarged by slightly modifying the configuration. A wavelength-tunable pump laser can be used, and the Brillouin fiber laser can be replaced by a probe laser at a fixed wavelength. By applying pump pulses at different wavelengths, each defining a unique measurable range of temperature in our setup, the total sensing range can be enhanced. Alternatively, the setup in Fig. 3 can also be directly applied to enlarge the measurable range of temperature simply by maintaining the Brillouin fiber laser cavity at different temperatures. Each selected temperature sets the reference for the starting point of a temperature sensing range.

Additional issues should be considered in practical application. Since the Brillouin gain spectrum is symmetric with respect to the gain peak, the increase and decrease of the temperature from room temperature will have the same effect on the delay, resulting in symmetric decrease of the time delay with respect to that of the room temperature [21], [22]. To determine the sign of temperature change, the system can work either along the rising slope or falling slope of SBS resonance by detuning the probe wavelength, instead of setting it at the peak gain. In addition, to decouple the effects of Brillouin frequency shift and pump power variation on the SBS delay, one may need to measure independently the received pump power at the opposite end of the fiber. Alternatively, a wavelength-tunable probe can be used to obtain a profile of the delay along the fiber at different wavelengths. A variation of pump power causes a proportional change in the SBS delay but the spectral peak position remains unchanged, whereas a temperature variation affects both the SBS delay and the peak position. For long distance sensing, there are several factors that should be considered. One of the factors would be the pump depletion or the excess amplification of the probe, which limits the sensing distance of the conventional Brillouin fiber sensor system [28], [29]. However, in our system, both the pump and probe are pulses. The two overlap with each other at the sensing point only once inside the fiber. Thus, the impact of the pump depletion or the probe amplification is alleviated. This is one advantage of our scheme. Another limiting factor is the delay tuning range of the electrical signal generator since large relative time delay between the pump and probe pulses is needed to monitor the remote sensing point along the fiber. Thus, a signal generator with large tuning range is desirable in long distance sensing. The third factor would be the fiber attenuation as it affects the pump power level and subsequently the probe pulse delay. For short distance real-time monitoring within hundreds of meters, the effect of fiber loss can be neglected. While for long distance (beyond tens of kilometers), in-line Raman amplifiers [5] may be used to compensate for the optical loss.

4. Conclusion

By measuring the SBS slow light delay of a probe pulse at different positions along the fiber, a new distributed temperature sensing scheme is realized. The scheme offers an alternative method of monitoring the temperature in a distributed manner, demonstrating the potential of real-time monitoring of specific positions in a short fiber link. The limitations of this scheme are also discussed and analyzed. The spatial resolution can be enhanced by using shorter pump and probe pulses, and higher temperature resolution is achievable with a stronger SBS pump and better control on the power stability.

References

[1] S. M. Maughan, H. H. Kee, and T. P. Newson, "57-km single-ended spontaneous Brillouin-based distributed fiber temperature sensor using microwave coherent detection," *Opt. Lett.*, vol. 26, no. 6, pp. 331–333, Mar. 2001.
[2] X. Bao, D. J. Webb, and D. Jackson, "32-km distributed temperature sensor based on Brillouin loss in an optical fiber," *Opt. Lett.*, vol. 18, no. 18, pp. 1561–1563, Sep. 1993.
[3] A. Minardo, R. Bernini, and L. Zeni, "Differential techniques for high-resolution BOTDA: An analytical approach," *IEEE Photon. Technol. Lett.*, vol. 24, no. 15, pp. 1295–1297, Aug. 2012.
[4] H. Liang, W. Li, N. Linze, L. Chen, and X. Bao, "High-resolution DPP-BOTDA over 50 km LEAF using return-to-zero coded pulses," *Opt. Lett.*, vol. 35, no. 10, pp. 1503–1505, May 2010.

[5] F. R. Barrios, S. M. López, A. C. Sanz, P. Corredera, J. D. A. Castañón, L. Thévenaz, and M. G. Herráez, "Distributed Brillouin fiber sensor assisted by first-order Raman amplification," *IEEE J. Lightw. Technol.*, vol. 28, no. 15, pp. 2162–2172, Aug. 2010.

[6] Y. Dong, L. Chen, and X. Bao, "Time-division multiplexing-based BOTDA over 100 km sensing length," *Opt. Lett.*, vol. 36, no. 2, pp. 277–279, Jan. 2011.

[7] R. Bernini, A. Minardo, and L. Zeni, "Stimulated Brillouin scattering frequency-domain analysis in a single-mode optical fiber for distributed sensing," *Opt. Lett.*, vol. 29, no. 17, pp. 1977–1979, Sep. 2004.

[8] A. Minardo, R. Bernini, and L. Zeni, "Brillouin optical frequency-domain single-ended distributed fiber sensor," *IEEE Sens. J.*, vol. 9, no. 3, pp. 221–222, Mar. 2009.

[9] K. Hotate and M. Tanaka, "Distributed fiber Brillouin strain sensing with 1-cm spatial resolution by correlation-based continuous-wave technique," *IEEE Photon. Technol. Lett.*, vol. 14, no. 2, pp. 179–181, Feb. 2002.

[10] M. Belal and T. P. Newson, "Enhanced performance of a temperature-compensated submeter spatial resolution distributed strain sensor," *IEEE Photon. Technol. Lett.*, vol. 22, no. 23, pp. 1705–1707, Dec. 2010.

[11] R. K. Yamashita, W. Zou, Z. He, and K. Hotate, "Measurement range elongation based on temporal gating in Brillouin optical correlation domain distributed simultaneous sensing of strain and temperature," *IEEE Photon. Technol. Lett.*, vol. 24, no. 12, pp. 1006–1008, Jun. 2012.

[12] M. G. Herráez, K. Y. Song, and L. Thévenaz, "Optically controlled slow and fast light in optical fibers using stimulated Brillouin scattering," *Appl. Phys. Lett.*, vol. 87, no. 8, p. 081113, Aug. 2005.

[13] Y. Okawachi, M. S. Bigelow, J. E. Sharping, Z. Zhu, A. Schweinsberg, D. J. Gauthier, R. W. Boyd, and A. L. Gaeta, "Tunable all-optical delays via Brillouin slow light in an optical fiber," *Phys. Rev. Lett.*, vol. 94, no. 15, pp. 153902-1–153902-4, Apr. 2005.

[14] M. G. Herráez, K. Y. Song, and L. Thévenaz, "Arbitrary-bandwidth Brillouin slow light in optical fibers," *Opt. Exp.*, vol. 14, no. 4, pp. 1395–1400, Feb. 2006.

[15] Z. Zhu, A. M. C. Dawes, D. J. Gauthier, L. Zhang, and A. E. Willner, "Broadband SBS slow light in an optical fiber," *IEEE J. Lightw. Technol.*, vol. 25, no. 1, pp. 201–206, Jan. 2007.

[16] K. Y. Song and K. Hotate, "25 GHz bandwidth Brillouin slow light in optical fibers," *Opt. Lett.*, vol. 32, no. 3, pp. 217–219, Feb. 2007.

[17] L. Thévenaz, K. Y. Song, and M. G. Herráez, "Time biasing due to the slow-light effect in distributed fiber-optic Brillouin sensors," *Opt. Lett.*, vol. 31, no. 6, pp. 715–717, Mar. 2006.

[18] A. Cheng, M. P. Fok, and C. Shu, "Wavelength-transparent, stimulated-Brillouin-scattering slow light using cross-gain-modulation-based wavelength converter and Brillouin fiber laser," *Opt. Lett.*, vol. 33, no. 22, pp. 2596–2598, Nov. 2008.

[19] A. E. Willner, B. Zhang, L. Zhang, L. Yan, and I. Fazal, "Optical signal processing using tunable delay elements based on slow light," *IEEE J. Sel. Topics Quantum Electron.*, vol. 14, no. 3, pp. 691–705, May/Jun. 2008.

[20] S. Chin and L. Thévenaz, "Optimized shaping of isolated pulses in Brillouin fiber slow-light systems," *Opt. Lett.*, vol. 34, no. 6, pp. 707–709, Mar. 2009.

[21] L. Wang, B. Zhou, C. Shu, and S. He, "Stimulated Brillouin scattering slow-light-based fiber-optic temperature sensor," *Opt. Lett.*, vol. 36, no. 3, pp. 427–429, Feb. 2011.

[22] L. Wang, B. Zhou, C. Shu, and S. He, "Temperature sensing using stimulated Brillouin scattering based slow light," presented at the Asia Communications Photonics Conference Exhibition (ACP 2010), Shanghai, China, Dec. 2010, paper FS6.

[23] R. Bernini, A. Minardo, and L. Zeni, "Dynamic strain measurement in optical fibers by stimulated Brillouin scattering," *Opt. Lett.*, vol. 34, no. 17, pp. 2613–2615, Sep. 2009.

[24] M. Nikles, L. Thévenaz, and P. A. Robert, "Simple distributed fiber sensor based on Brillouin gain spectrum analysis," *Opt. Lett.*, vol. 21, no. 10, pp. 758–760, May. 1996.

[25] G. P. Agrawal, *Nonlinear Fiber Optics,* 4th ed., Singapore: Elsevier, 2009.

[26] A. Zadok, S. Chin, L. Thévenaz, E. Zilka, A. Eyal, and M. Tur, "Polarization-induced distortion in stimulated Brillouin scattering slow-light systems," *Opt. Lett.*, vol. 34, no. 16, pp. 2530–2532, Aug. 2009.

[27] L. Wang and C. Shu, "Demonstration of distributed strain sensing with the use of stimulated Brillouin scattering-based slow light," *IEEE Photon. J.*, vol. 3, no. 6, pp. 1164–1170, Dec. 2011.

[28] L. Thevenaz, S. F. Mafang, and J. Lin, "Impact of pump depletion on the determination of the Brillouin gain frequency in distributed fiber sensors," in *Proc. SPIE*, 2011, vol. 7753, pp. 775322-1–775322-4.

[29] X. Bao, H. Liang, Y. Dong, W. Li, Y. Li, and L. Chen, "Pushing the limit of the distributed Brillouin sensors for the sensing length and the spatial resolution (Invited Paper)," in *Proc. SPIE*, 2010, vol. 7677, p. 767702.